**JAST**, Vol. 14, No 1, pp 103-110


JAST
Journal of Aerospace Science and Technology

# Science Article

# Experimental Investigation of using Plasma Actuators as Virtual Gurney Flap

Bahareh Mojarrad[1], Saeed Oveisi[2], Mostafa Kazemi[3], Mahmoud Mani[4*]
1-DANA Aerodynamic Laboratory, Amirkabir University of Technology
2,3,4 Faculty of Aerospace Engineering, Amirkabir University of Technology
* Code; 15875-4413,Hafez Street, Tehran
Email: *mani@aut.ac.ir

*The primary objective of this study was to demonstrate how plasma actuators could be used to discharge a perpendicular dielectric barrier as a virtual Gurney flap. This study utilized wind tunnel experiments on a flat plate airfoil. Each experiment is conducted at two different free flow velocities of ten and twenty meters per second. To study and extract the aerodynamic phenomena generated by plasma actuators and to compare them to the Gurney phenomena of a physical flap, velocity profiles in the model sequence were measured using a hot wire flow meter in two different longitudinal positions relative to the model. All experiments were conducted from five distinct vantage points, 0, 2, 4, 6, and 8, and plasma actuators were activated in two distinct settings to extract concepts under a variety of conditions. Wind tunnel experiments indicate that downward sequence transfer occurs when plasma actuators are used. Additionally, there are two distinct types of vortex shedding on the model's back: one that resembles Karman vortex shedding and another that occurs below the model. The observation of velocity profiles demonstrates that the deformation of the sequence caused by the use of plasma actuators is very similar to that caused by an airfoil sequence equipped with a physical Gurney flap.*

**Keywords:** *Flow control, plasma actuators, wind tunnel, virtual Gurney flap, hot wire flow meter.*

## Introduction

Due to advancements in aerospace engineering and the relative stability of the overall shape of flying objects over the last few decades, flow control has become a critical component of aerodynamics. Among the most critical objectives of flow control are the correction of flow patterns, the increase of lift force, and the decrease of drag force. The progress and development of flow control methods over the last century demonstrate its significance [1]. Flow control is the process of actively or passively modifying a fluid to effect the desired change [2]. In other words, flow control refers to any process that alters the behavior of a fluid from its natural state [3]. Williams and McMinowski have historically classified flow control as belonging to the "experimental era" or the "modern era." According to them, while flow control was achieved during the experimental era by consuming a significant amount of energy, the primary goal in the modern era is to affect the structure of the fluid with the least amount of energy. This is accomplished by exploiting the instabilities of fluids as an actuator. In general, the primary distinction between experimental and

1 MSc Student
2 PhD Student
3 PhD Student
4 Professor (Corresponding Author)

Received: 18 July 2021
Accepted: 19 Oct. 2021

modern eras of flow control is the amount of energy required to affect the same variations [4]. The use of Gurney flaps to increase the aerodynamic efficiency of various types of wings and airfoils is one method of passive flow control. As illustrated in Figure 1, this device is a straightforward appendage perpendicular to the flow at the airfoil's end. In the 1960s, Daniel Gurney pioneered the use of the Gurney flap in racing cars to achieve lift [5]. Due to the presence of this appendage at the airfoil's end, a vortex is created in front of and below the airfoil, as well as two vortices behind it. According to Joukowski's principle, the vortex beneath the airfoil alone increases the lift in the wing and introduces negative twisting moments into the airfoil. Additionally, the two vortices behind the Gurney flap alter the quota condition at the trailing edge. Additionally, due to the low pressure and suction zone at the airfoil's end, there is increased adhesion in this region. Liebeck et al. [6] Pioneered the use of this type of flow control device on airfoils, demonstrating through a series of experiments that by varying the height of the Gurney flap, the lift coefficient can be increased by approximately 50%. Then, researchers examined a variety of variables to conduct several studies on Gurney flap use and efficiency. Effects of changes in height [7-9], change in the installation angle [10-11], alternate location [10], and Gurney flap shape [12-13], have been the variables examined.

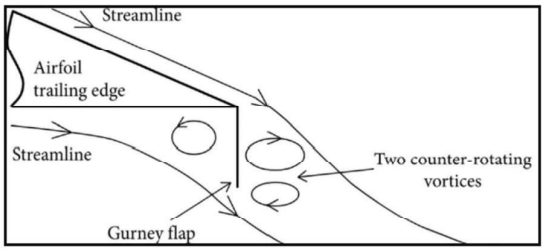


**Fig. 1.** Flow diagram around Gurney flap and how to install it on airfoil with vortex in flows [14].

When it comes to active flow control, it can be said that in the last decade, the use of plasma discharge actuators dubbed Dielectric Barrier Discharge (DBD) as one of the active flow control methods has become quite common. The technology was initially used to reduce the flat plate drag coefficient in the late twentieth century, and then Roth developed DBD [15-16]. These actuators quickly gained widespread use in aerodynamics due to their numerous advantages, including the absence of a moving part, extremely low weight, rapid response time in the unstable state, and adaptability to a variety of surfaces [17]. As illustrated in Fig. 2, the DBD actuator is composed of two electrodes: an exposed electrode and an embedded electrode. An insulating material separates the two electrodes. The coefficient of the insulation material used to construct the DBD actuator, as well as its thickness, are critical factors in plasma formation. The most frequently used insulation materials are a type of polyamide known as Kapton and a type of Teflon known as TPFE [18]. When electrodes in DBD actuators are supplied with an alternating flow with a sufficiently high voltage and flow intensity, they ionize a very thin layer of air molecules (typically less than one part per million) in their vicinity. According to the classical view, ionized gas is a type of plasma, which is why this type of actuator is called a plasma actuator [19].

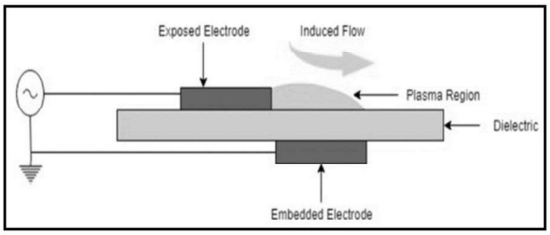


**Fig. 2.** Scheme of DBD components.

The presence of an electric field generated by the electrodes, which varies in shape, results in the entry of volumetric force into the air molecules. Kriegseis summarizes the applications and highlights in the field of DBD and boundary layer control in a review article [20]. According to wind tunnel tests, the Gurney flap's optimal dimensions are between 1% and 2% of the airfoil chord. However, when flying, the same 1 to 2% flap can significantly increase the drag force. A Gurney flap should be designed for this purpose that can be used only when necessary, such as on a cruise flight. However, developing such a mechanism is extremely difficult. A virtual Gurney flap is an alternative. A virtual Gurney flap can be created using a variety of fluid, synthetic, or atmospheric cold plasma jets. Experiments with virtual Gurney flaps demonstrate that the use of fluid jets can improve coefficients of lift and can be used in place of mechanical flaps. This way, the flap can be activated only when necessary, avoiding the production of unnecessary lift. The use of electric barrier discharge plasma is one method of producing fluid jets. This method simulates the

effect of the flap and activates it only when necessary. The primary objective of this study is to determine whether the Gurney mechanical flap can be virtually simulated. This research utilized one of the most advanced active flow control techniques available today, plasma dielectric barrier discharge. This project's primary objective is to investigate the effect of transverse or vertical plasma blow on free flow. The study examined the effect of adding DBD actuators on the shape of the flow sequence as measured by a hot wire flow meter on a flat plate model and at two different velocities. At attack angles of 0, 2, 4, 6, and 8 degrees, the shape of the model sequence is examined to determine how the velocity profile changes over time. It is possible to determine the extent to which the flow field has changed by examining the data obtained from the flow field in the conclusion of the model, which is similar to the model sequence for the flat plate equipped with a mechanical Gurney flap.

## Methodology and the Tools of the Experiment

A flat-panel airfoil model with a 42 cm chord, 46 cm aperture, and 23 mm thickness was used in this research. At the start of the model, a wedge with a length of 14 cm and a vertex angle of 10 degrees is installed to prevent the flow from abruptly separating from the model's attack edge and to ensure that the boundary layer which is on the flat plate has the correct shape. Additionally, the declared chord includes the model's length defined from the edge of the wedge to the model's end. Only one dielectric plasma actuator is mounted on the model's trailing edge. This actuator is configured in such a way that the generated induced flow (or plasma flow) is perpendicular to the free flow. The explicit and implicit electrodes are made of copper with a thickness of 0.1 mm, and a 5 mm thick plexiglass plate acts as a dielectric between them. The actuator was the width of the airfoil aperture, 5.2 mm in height, and 2 mm in length. The actuator schema that is developed is depicted in Fig. 3. Additionally, this figure shows the image of the actuator that is generated.

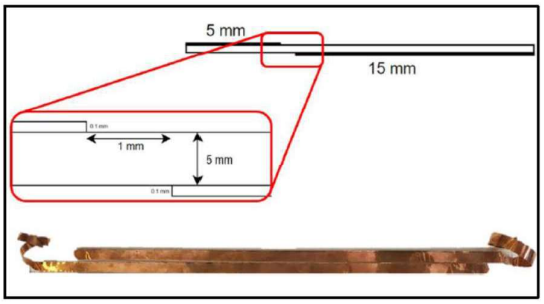


**Fig. 3**. Plasma actuator dimensions and its image.

The experiments were conducted at speeds of ten and twenty meters per second and in two distinct categories of electrical discharge environments:
Voltage: 8 kV, frequency: 6 kHz,
Voltage: 10 kV, frequency: 8 kHz.
The speed profile was quantified in two distinct sections at velocities of 10 and 20 meters per second. The chosen voltage and frequency are examined in both cases at attack angles of 0, 2, 4, 6, and 8 degrees. The effects of plasma presence on the flow field can be observed by comparing the shape of the flow sequence in the absence of plasma to the shape of the flow sequence in the presence of plasma. All experiments were conducted in Amirkabir University of Technology's infrasound wind tunnel (Tehran Polytechnic). This open-circuit suction wind tunnel features a rectangular test section with a volume of 1*1*1.8 cubic meters and a speed range of 2.5 to 60 meters per second. The intensity of wind tunnel disturbances in the test section is less than 0.1 percent when using a nozzle with a density ratio of 9 to 1, a honeycomb layer, and three mesh layers. To control the wind tunnel's velocity, a Kimo Company digital micro manometer, model MP120, was used. This instrument is capable of measuring the wind tunnel's velocity with an accuracy of 0.1 meters per second. A hot wire flow meter, which operates at a constant temperature, was used to determine the flow velocity in the sequence. The diameter of the hot wire flowmeter probes is 6 mm, and the distance between the collars is 4 mm. The distance between the collars is determined by welding a 5-micron tungsten wire at a constant temperature of 400° C. Traverses are used to move the hot wire probe between wind tunnel positions, and the device can move with a 1 mm accuracy in three different directions. An alpha-mechanism has been used to change the angle of attack of the model. This device, which utilizes a powerful stepper motor and predicted

mechanisms, is capable of accurately adjusting the angle of attack of the model inside the tunnel to within 0.05%, putting it in the category of precision instruments. Fig. 4 depicts the wind tunnel diagram and test instruments. Additionally, Table 1 contains a list of all variables examined in this study. To determine the uncertainty of the proposed velocity profiles and the amount of measurement error, the accuracy values of various devices (Kimo speedometer and hot wire flow meter) were compared to the hot wire calibration method modified by King with variable power n. At the measured velocities, an error of 0.54 percent is obtained. Naturally, it should be noted that during the iteration of experiments, a difference in the reproducibility of the results of 0.8 percent was observed; because this difference is greater than the calculated error, the reproducibility value is introduced as a test error and all velocity numbers are recalculated. The velocity profiles depicted in this study have an error rate of 0.8%, and variations within this range are considered unacceptable.

**Table 1**. Studied Variables.

| Studied Variable | Values |
|---|---|
| Free flow velocity | 10 and 20 m/s |
| Plasma setting 1 | Voltage: 8 kV, frequency: 6 kHz |
| Plasma setting 2 | Voltage: 10 kV, frequency: 8 kHz |
| Distance from trailing edge | 10 and 20 mm |
| Angle of the attack | 0, 2, 4, 6, and 8 degrees |

## Results

The velocity profile data from the model sequence are analyzed in this section at two horizontal distances of 10 and 20 mm from the trailing edge. As previously stated, the study will examine attack angles of 0, 2, 4, 6, and 8 degrees. The speed diagrams for 10 m/s and the effect of increasing the angle of attack on the sequence profile are presented first, followed by the speed diagrams for 20 m/s and the effect of increasing the angle of attack on it. On the other hand, each diagram illustrates the effect of two different sets of plasma excitation regulations that are comparable to the off-plasma mode. Additionally, attempts have been made to explain the sequence and flow field behavior at the model's conclusion in order to compare the flow's physical similarity to an airfoil equipped with mechanical Gurney flaps.

The sequences are presented in the profile with an increasing angle of attack at a distance of 10 mm. The attack angle has been increased to 8 degrees from left to right. In the absence of plasma, the sequence of the material is symmetrical at a zero-degree angle of attack and at the shortest measured distance. This symmetry is unmistakably due to the geometry's symmetry and the absence of an attack angle. At the top and bottom of the sequence, when the plasma begins to operate, two significant phenomena are visible. Dynamic pressure increased nearly symmetrically prior to and following the dynamic pressure drop zone. The presence of this phenomenon in the sequence can be interpreted as velocity induction perpendicular to the flow. Indeed, the fluid flow tends to rotate downward when the plasma actuator is activated. This rotation results in the induction of velocity parallel to the flow, thereby increasing the velocity and dynamic pressure. Bypassing through this region and approaching the axis of symmetry, the effect of increasing dynamic pressure gradually diminishes and the effect of the material increases, resulting in a reduction in flow velocity.

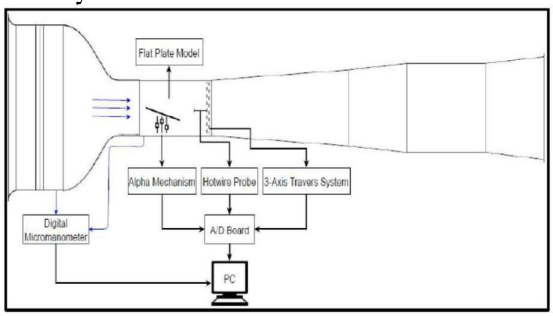


**Fig. 4.** Wind tunnel scheme and experiment tools

When the plasma stimulator is turned on, the velocity values decrease significantly. In general, the amount of drag force can be predicted to have increased. Because areas of the dynamic pressure increase are generally smaller than areas of dynamic pressure decrease when actuators are activated. However, because the measuring point is close to the body, this sequence cannot be used to determine the drag force at a distance of 10 mm. As the drag force is calculated using only the component parallel to the current. However, because of the high rotation of the flow in this location, the velocity components in the direction perpendicular to the flow cannot be ignored. On

the other hand, because one-dimensional measurements are performed using a hot wire, velocity values in the direction of the current cannot be determined.

As the plasma is activated, the increase in dynamic pressure drop is equivalent to the increase in the power of the dorsal vortices. As can be seen, with plasma activation, the behavior associated with the presence of continuous vortices in the sequence has increased. Additionally, the distance between the peaks in the diagram corresponding to the second plasma setting has increased slightly.

Moving in the direction of flow and considering Fig. 6 at a zero-degree angle of attack and a distance of 20 mm, it is clear that the behavior of interconnected peaks quickly vanishes at this velocity and distance from the model's end. On the other hand, the absence of plasma has resulted in an expansion of the sequence. Active actuator sequences do not affect dynamic pressure, as illustrated in Fig. 6. On the other hand, these sequences began later and ended sooner than those lacking plasma. The effect of interconnected peaks appears to have vanished, based on the data collection points. Additionally, the diagrams differ less than those in Fig. 5, indicating that the effect of changes in plasma voltage and frequency has diminished more rapidly in such sequences.

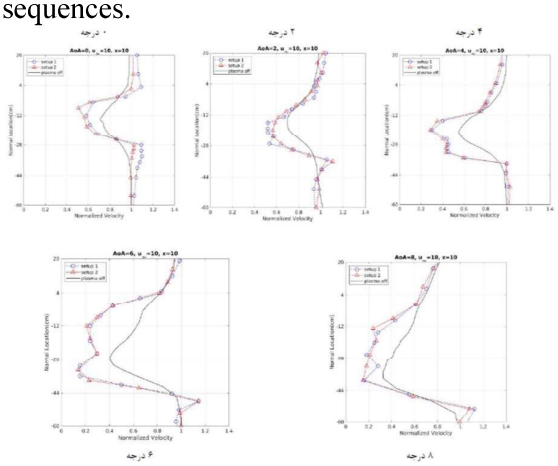

**Fig. 5**. Velocity profiles in the sequence at a distance of 10 mm, velocities of 10 m/s, attack angles of zero to 8° and two different plasma settings compared to off-plasma.

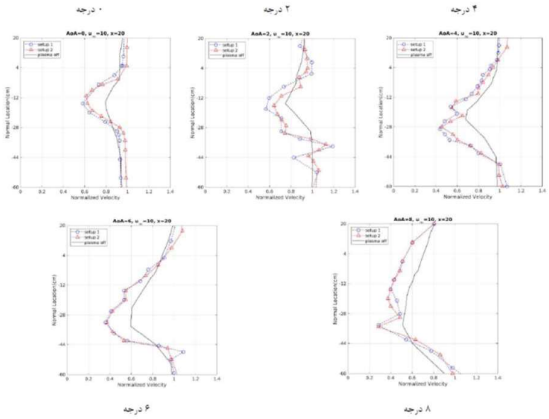

**Fig. 6**. Velocity profiles in the sequence at a distance of 20 mm, velocities of 10 m/s, attack angles of zero to 8° and two different plasma settings compared to off-plasma.

By examining the shape of the sequence at a distance, it is clear that it is significantly wider than it was previously for the off-plasma mode. As previously stated, widening of the sequence is expected due to momentum diffusion. Additionally, it can be seen that clear plasma sequences exhibit a double-peak behavior. This indicates the presence of small vortices at this distance. As a result, the behavior of the double-peak can probably be observed at a distance of 20 mm. The inability to observe such a phenomenon could be a result of a dearth of data collection points.

To begin, this section illustrates the profile shape of the sequences at a distance of ten millimeters with an increasing angle of attack. According to Figure 7, the angle of attack has increased to 8 degrees from left to right. At a zero-degree angle of attack and a distance of 10 mm, the body sequence is symmetric because the model is symmetric. The presence of plasma before and after the dynamic pressure drop zone has resulted in a relatively symmetrical increase in dynamic pressure. This could be due to the plasma actuator inducing velocity perpendicular to the flow, which directed the flow downward. The dynamic pressure has been increased by inducing velocity perpendicular to the flow and increasing velocity in this direction. Near the symmetry axis, the effect of increasing dynamic pressure gradually diminishes, while the effect of the model's vortices increases. The effect of increasing the dynamic pressure decreases as the angle of attack increases up to 2 degrees, and there is no effect at all in the first plasma settings.

As the plasma actuator is activated, the velocity values decrease more rapidly and the areas of dynamic pressure increase become smaller than the areas of the dynamic pressure decrease, implying an increase in drag. However, because the measuring point is close to the body, it is incorrect to use this sequence to determine the drag force at a distance of 10 mm. Because the drag force should be calculated using only the parallel component of the flow. When the plasma actuator is activated, the rotation in the final half of the sequence increases, and the velocity component perpendicular to the flow direction can no longer be ignored. As the plasma is turned on, the increase in dynamic pressure drop is equivalent to the increase in the power of the dorsal vortices. As can be seen, plasma activation enhances the behavior of twin and continuous vortices in the sequence, resulting in sequence diagram deformation.

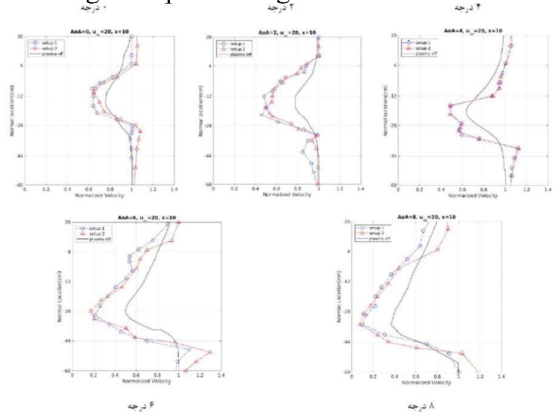

**Fig. 7.** Velocity profiles in the sequence at a distance of 20 mm, velocities of 10 m/s, attack angles of zero to 8° and two different plasma settings compared to off-plasma.

Moving in the direction of flow and considering Figure 8 at a zero-degree angle of attack and a distance of 20 mm, it is clear that increasing the velocity and distance from the model's end reduces the effect of interconnected peaks in the sequence. As illustrated in the figure, active actuator sequences do not increase dynamic pressure. However, these sequences began later and ended earlier than those without plasma. According to the data collection points, it appears as though the effect of interconnected peaks has been eliminated. Additionally, the diagrams are less distinct than those in the preceding figure, indicating that the effect of plasma voltage and frequency changes in such sequences has waned rapidly. According to the figure, the first set of plasma with an 8-kW voltage and a frequency of 6 kHz was able to bend the peak of the sequence down further, whereas the second set with a 6-kW voltage and an 8 kHz frequency had no such effect.

Furthermore, it is visible that clear plasma sequences exhibit a double-peak behavior. This demonstrates that at this distance, small vortices exist. Thus, at a distance of 20 mm, the behavior of interconnected vortices can most likely be observed. The inability to observe such a phenomenon could be a result of a lack of data collection points.

## Conclusion

Aeronautical science considers the flow around a flat plate to be one of the fundamental flows. Despite its simplicity in the geometry under analysis, this flow can determine a great deal about the flow in general. As such, if it is consistent with the circumstances surrounding the issues under consideration, it will be considered a first choice. The primary objective of this study was to determine the effect of a plasma actuator's vertical blow on the flow around a flat plate. The purpose of this study is to investigate and evaluate the possibility of using perpendicularly biased plasma actuators at the airfoil's end as a virtual Gurney flap. Gurney flaps are among the most efficient and straightforward types of flaps and surfaces. However, there are some limitations to the use of this flap. The primary shortcoming of these flaps is their inability to perform well in cruise flight conditions. These flaps are intended for use during landing and takeoff only. On the other hand, structural flaws prevent these flaps from being used exclusively during take-off and landing. Due to the difficulties inherent in operating this flap, one of the challenges is the possibility of operating it optimally and removing it from the geometry. It is undesirable in certain circumstances. However, using Gurney flaps is nearly impossible. Among the proposed solutions is the use of virtual Gurney flaps. The decade used in this study is the sequence of the flow perpendicular to the distant current. Understanding the action of a plasma actuator in simpler cases is critical in the initial stages of research on such a concept. As a result, the identical problem is located at the bottom of the flat plate being studied. In this study, a simple flat plate was first tested in a wind tunnel. This plate was then fitted with plasma actuators, and the effects of plasma presence at two voltages and frequencies were investigated.

The data were collected using a hot wire flow meter at two different distances from the model's trailing edge. The experiments were conducted at two different speeds of ten and twenty meters per second and attack angles of zero, two, four, six, and eight degrees. At each point, velocity profile diagrams demonstrate that the presence of plasma has deformed the sequence. When the plasma is turned on, the shape of the sequences is slightly shifted to the lower extremities. Additional behaviors are visible. To begin, there is a phenomenon in sequences referred to as contiguous vortices in this text. Gurney flap sequences are another manifestation of this phenomenon. Second, the sequences contain an inverse peak that lies below the model (the direction in which the plasma actuator was directed). These peaks denote an increase in velocity in the model's lower regions.

Another significant point in the form of a sequence is the reflection of the shape of the sequences for states of plasma presence relative to states of plasma absence. By increasing the angle of attack, one could almost argue that the shape of the sequence appears more prominently in the presence of plasma and in the absence of difference at close distances. As a result, the effects are expected to increase as the angle of attack increases. However, with a triple resistance between the 6- and 8-degrees angles, it appears as though the effects at the 8-degrees angle have decreased again. It should be noted that all results are considered in aggregate and that some processes make exceptions. These trends, however, can be generalized to a single conclusion. In summary, this study's findings indicate that:

1. Applying the blowing flow with the plasma in a perpendicular direction to the flow can result in a deformation of the sequence similar to the effect of Gurney flaps on an airfoil's sequence. These modifications include a very slight downward shift in the sequence and the formation of interconnected (twin) vortices.
2. In this configuration, the plasma actuator produces a series of phenomena that result in a slight increase in velocity.
3. When plasma actuators are used, the vortex passage is slightly curved downward. If the remote flow has a high velocity, the distance between the vortices will slightly increase rather than bending downward.

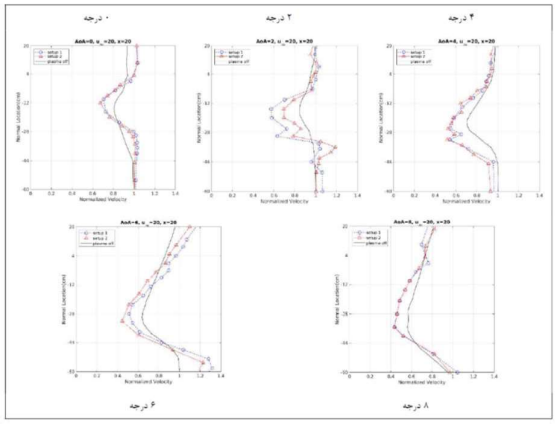

**Fig. 8.** Velocity profiles in the sequence at a distance of 20 mm, velocities of 20 m/s, attack angles of zero to 8° and two different plasma settings compared to off-plasma.

## Reference

[1] S. Joshi and Y. Gujarathi, "A review on active and passive flow control techniques," International Journal on Recent Technologies in Mechanical and Electrical Engineering, vol. 15, no. 1, pp. 16-22, 2014.

[2] M. Gad-el-Hak, "Flow Control: Passive, Active, and Reactive Flow Management. 2000," ed: Cambridge University Press.

[3] J. Flatt, "The history of boundary layer control research in the United States of America," Boundary Layer and Flow Control, vol. 1, pp. 122-143, 1961. [4] R. D. Joslin and D. N. Miller, Fundamentals and applications of modern flow control. American Institute of Aeronautics and Astronautics, 2009.

[5] J. Wang, Y. Li, and K.-S. Choi, "Gurney flap—Lift enhancement, mechanisms and applications," Progress in Aerospace Sciences, vol. 44, no. 1, pp. 22-47, 2008.

[6] R. H. Liebeck, "Design of subsonic airfoils for high lift," Journal of aircraft, vol. 15, no. 9, pp. 547-561, 1978.

[7] Y. Li, J. Wang, and P. Zhang, "Effects of Gurney flaps on a NACA0012 airfoil," Flow, Turbulence and Combustion, vol. 68, no. 1, p. 27, 2002.

[8] P. Giguere, G. Dumas, and J. Lemay, "Gurney flap scaling for optimum lift-to-drag ratio," AIAA journal, vol. 35, no. 12, pp. 1888-1890, 1997.

[9] F. Ajalli and M. Mani, "Effects of adding strip flap on a plunging airfoil," Aircraft Engineering and Aerospace Technology: An International Journal, 2014.

[10] Y. Li, J. Wang, and P. Zhang, "Influences of mounting angles and locations on the effects of Gurney flaps," Journal of Aircraft, vol. 40, no. 3, pp. 494-498, 2003.

[11] L. W. Traub, A. C. Miller, and O. Rediniotis, "Preliminary parametric study of Gurney flap dependencies," Journal of aircraft, vol. 43, no. 4, pp. 1242-1244, 2006.

[12] D. H. Neuhart and O. C. Pendergraft Jr, "A water tunnel study of Gurney flaps," 1988.

[13] Y.-C. Li, J.-J. Wang, and P.-F. Zhang, "Experimental investigation of lift enhancement on a NACA 0012 airfoil using plate/serrated Gurney flaps," Acta Aeronautica et Astronautica Sinica, vol. 24, no. 2, pp. 119-123, 2003.

[14] L.-S. Hao and Y.-W. Gao, "Effect of Gurney Flap Geometry on a S809 Airfoil," International Journal of Aerospace Engineering, vol. 2019, 2019.
[15] S. El-Khabiry and G. M. Colver, "Drag reduction by dc corona discharge along an electrically conductive flat plate for small Reynolds number flow," Physics of fluids, vol. 9, no. 3, pp. 587-599, 1997.
[16] J. Roth, D. Sherman, and S. Wilkinson, "Boundary layer flow control with a one atmosphere uniform glow discharge surface plasma," p. 328.
[17] T. Corke and M. Post, "Overview of plasma flow control: concepts, optimization, and applications," p. 563.
[18] R. E. Hanson, N. M. Houser, and P. Lavoie, "Dielectric material degradation monitoring of dielectric barrier discharge plasma actuators," Journal of Applied Physics, vol. 115, no. 4, p. 043301, 2014.
[19] M. P. Patel et al., "Scaling effects of an aerodynamic plasma actuator," Journal of aircraft, vol. 45, no. 1, pp. 223-236, 2008.
[20] J. Kriegseis, B. Simon, and S. Grundmann, "Towards in-flight applications? a review on dielectric barrier discharge-based boundary-layer control," Applied Mechanics Reviews, vol. 68, no. 2, p. 020802, 2016.